Journal of Superconductivity and Novel Magnetism (2023) 36:685–692
https://doi.org/10.1007/s10948-023-06510-x

ORIGINAL PAPER

Relationship Between the Magnetization and Resistivity of Typical Magnetic Materials

Z. Z. Li[1] · W. H. Qi[1] · L. Ma[1] · G. D. Tang[1,2] · G. H. Wu[2] · F. X. Hu[2]

Received: 18 October 2022 / Accepted: 17 January 2023 / Published online: 10 February 2023

Abstract
Based on several reports presented valence electron structure experimental results since the 1970s, a set of new itinerant electron models for typical magnetic materials were proposed to replace the conventional exchange interaction models. According to the new models, in this article, we investigate the temperature dependence relationship between the magnetization and resistivity of typical magnetic materials. At the ground state, valence electrons of the outer shell in an ion (or in an ionic core in a metal) move in a constant spin direction. When two approaching electrons with the same spin direction belong to two adjacent ions, they can exchange each other, to form itinerant electrons. When two approaching electrons with opposite spin directions belong to two adjacent ions, they cannot exchange each other; as a result, a Weiss electron pair (WEP) is formed with a specific probability and lifetime. The energy of WEPs serves as the origin of the magnetic ordering energy. With temperature increments, the spin direction of the itinerant electrons deviates from the ground state direction, increasing the resistivity of the materials; the spin directions of the electrons in a WEP deviate from the ground state direction, resulting in the magnetic ordering energy decreasing and, meanwhile, a decrease in the magnetization.

Keywords Magnetic material · Magnetization · Resistivity · Itinerant electron · Magnetic ordering energy

1 Introduction

The magnetic and electrical transport properties of typical magnetic metals, iron (Fe), cobalt (Co), and nickel (Ni), as well as relative alloys, and the manganites $R_{1-x}T_xMnO_3$ with an ABO_3 perovskite structure (where R and T are rare earth and alkaline earth ions, respectively), have been extensively studied using conventional magnetic ordering models, including exchange interaction model for magnetic metals, double exchange interaction model, and superexchange interaction model for magnetic oxides [1–4]. However, no report based on valence electron structure was found for the relationship between the magnetization and resistivity of typical magnetic materials. Obviously, both magnetic and electrical transport properties are related to the valence electron structure of the materials. Therefore, on the basis of valence electron structure, to research the relation between magnetic and electrical transport properties is not only a feasible path, but also may benefit to understand the physical mechanism of magnetic and electrical transport phenomena.

Since the 1970s, many experimental results on valence electron states have been reported that provide bases for resolving the difficulties related to the magnetic ordering phenomena faced by conventional magnetic ordering models, resulting in a set of new itinerant electron models [5–11]. The new models include an O 2*p* itinerant electron model for magnetic oxides (the IEO model), a new itinerant electron model for magnetic metals (the IEM model), and a Weiss electron-pair (WEP) model for the origin of the magnetic ordering energy of both magnetic metals and oxides (see Appendices 1 – 3). Using these models, the magnetic ordering phenomena of several series of typical magnetic materials were explained [5, 6], including magnetic ordering experimental phenomena, based on the conventional models, as well as several experimental phenomena that have been the topic of ongoing disputes

✉ G. D. Tang
tanggd@hebtu.edu.cn

[1] Hebei Advanced Thin Film Laboratory, Department of Physics, Hebei Normal University, Shijiazhuang City 050024, People's Republic of China

[2] State Key Laboratory of Magnetism, Institute of Physics, Chinese Academy of Sciences, Beijing 100190, People's Republic of China

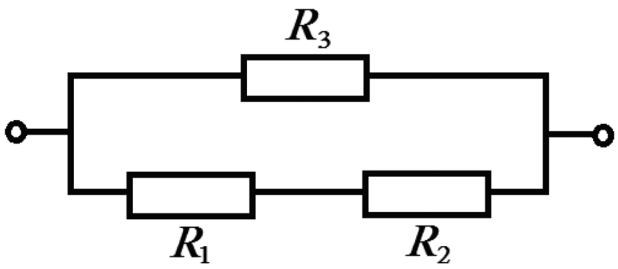

Fig. 1 An equivalent circuit with two current-carrier channels, used to fit the dependencies of resistance R on test temperature T. R_1 and R_2 are in the spin-dependent channel of the IEs for both magnetic metals and oxides below T_C. R_3 is in the spin-independent channel of the FEs for magnetic metals or the IEs for oxides [12, 13]

for many years. Based on these new magnetic ordering models, the temperature dependences of the resistivity for a series of single-crystal manganites, i.e., $La_{1-x}Sr_xMnO_3$ with an ABO_3 perovskite structure, and a set of $Ni_{1-x}Cu_x$ alloys were fitted using an equivalent device with two current-carrier channels [12, 13].

In order to understand the physics mechanism related to valence electron structure of magnetic and electrical transport of the magnetic materials, in this article, using the new itinerant electron models, we discuss the relationships between the magnetization and resistivity of magnetic metals, Fe, Co, and Ni, alloys $Ni_{1-x}Cu_x$, and manganites $La_{1-x}Sr_xMnO_3$. These materials are typical magnetic materials, whose magnetic and electrical properties have been researched extensively, but the relationship between the resistivity and magnetization has not been reported. First, we fit the temperature dependences of the resistivity of the materials using an equivalent device with two current-carrier channels; then, we discuss the temperature dependences of the magnetizations using the parameters obtained from the resistivity fitting process. The experimental data used in the fitting process comes from the references.

2 Fitting the Temperature Dependences of the Resistivity for Fe, Co, and Ni Magnetic Metals and $Ni_{1-x}Cu_x$ Alloys

According to the IEM model [5, 6, 9], valence electrons have the following characteristics. (i) In the formation process of a 3*d* transition metal (excluding copper and zinc with a full 3*d* electron shell) from free atoms, most of the 4*s* electrons entered the 3*d* orbits of the ionic core (called the "ion" or "cation" in next), while the remaining 4*s* electrons formed free electrons (FEs). (ii) The movement of FEs is subjected to the weak crystal-lattice potential field but not to the electron orbits, the spins of which do not contribute to the ion magnetic moment. (iii) The electrons in the outer orbit of an ion can transit with a specific probability to the outer orbit of an adjacent ion, forming itinerant electrons (IEs); other valence electrons are local electrons (LEs). The transition of IEs with a constant spin direction is spin-dependent below the Curie temperature (T_C) but is spin-independent above the T_C; the spins of the IEs have a similar contribution to those of LEs to the ion magnetic moment.

Accordingly, the resistivity (i.e., ρ) curves vs. the test temperature (T) of magnetic metals and alloys may be fitted using an equivalent device with two current-carrier channels [13], as shown in Fig. 1. In this figure, R_3 represents the resistance (resistivity ρ_3) originating from the FEs, which are scattered by a weak, periodic crystal-lattice potential field; R_1 represents the resistance (resistivity ρ_1) originating from the transition of the IEs between adjacent ions, which are scattered by the crystal lattice; R_2 represents the resistance (resistivity ρ_2) originating from the IEs, the spin direction of which deviate rapidly from the ground state direction when the T is close to the T_C. Therefore, the total resistance, i.e., R, in Fig. 1 can be calculated using the following equation:

$$R = \frac{(R_1 + R_2)R_3}{R_1 + R_2 + R_3}$$

Relative resistivity is represented by

Table 1 Fitted parameters of curves of the resistivities, ρ_1, ρ_2, ρ_3, versus test temperature, T, for Fe, Co, and Ni metals and $Ni_{1-x}Cu_x$ alloys, where $\rho_1 = (a_{11} + a_{12}T)^3$, $\rho_1 = a_2 \exp\left(-\frac{E_2}{k_B T}\right)$, $\rho_3 = \rho_0 + a_3 T$

Materials	a_{11} [(μΩ cm)$^{1/3}$]	a_{12} [(μΩ cm K^{-1})$^{1/3}$]	a_2 (μΩ cm)	E_2 (eV)	T_C (K)	ρ_0 (μΩ cm)	a_3 (μΩ cm K^{-1})
Co	0.90	3.7×10^{-3}	6.0×10^{7}	1.30	1404	50.0	0.0300
Fe	1.00	4.5×10^{-3}	1.50×10^{9}	1.30	1043	84.0	0.0230
Ni	0.60	5.7×10^{-3}	4.5×10^{12}	1.30	631	15.1	0.0230
$Ni_{90.39}Cu_{9.61}$	1.05	8.5×10^{-3}	7.0×10^{12}	1.03	522	25.8	0.0230
$Ni_{80.46}Cu_{19.54}$	1.60	1.15×10^{-2}	1.7×10^{13}	0.85	415	35.5	0.0185

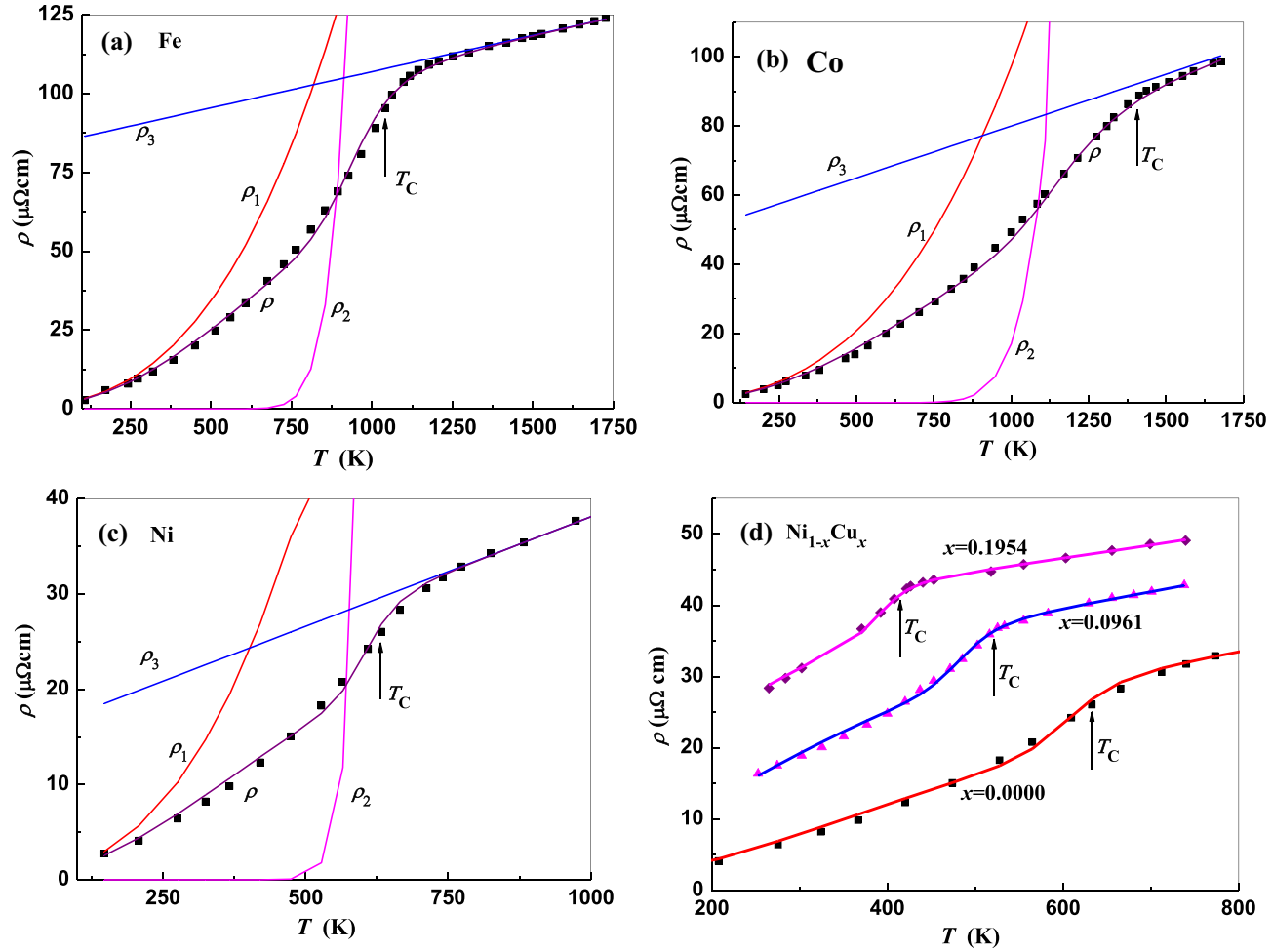

Fig. 2 Temperature dependence of resistivity ρ of polycrystalline materials, where the curves represent the fitted results in this work, the points represent the observed results. The observed data of Fe (**a**), Co (**b**), and Ni (**c**) originated from Reference [14]; the observed data of $Ni_{1-x}Cu_x$ ($x = 0.0961, 0.1954$) alloys (**d**) taken from Reference [15]

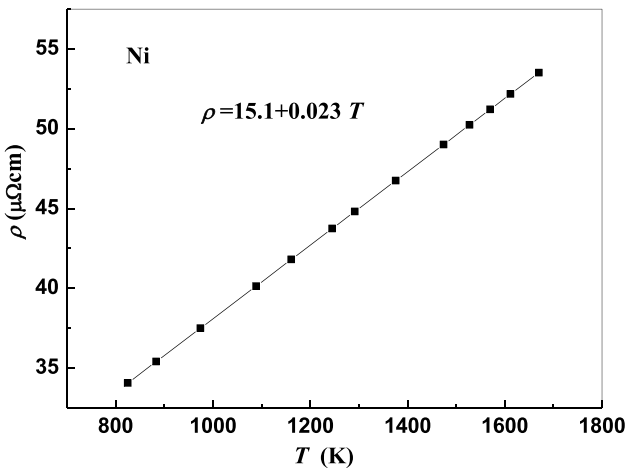

Fig. 3 A linear fitting for the curve of resistivity ρ versus temperature T for Ni at the high temperature region. Where the points are observed values [14], the line is the fitted result

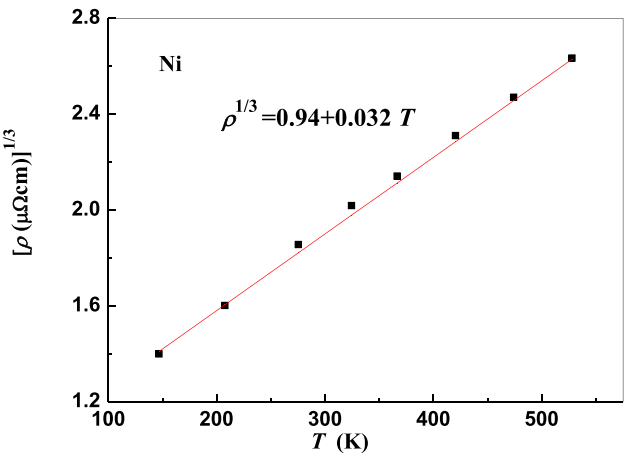

Fig. 4 A linear fitting for the curve of $\rho^{1/3}$ versus temperature T for Ni at the low temperature region. Where the points are observed values [14], the line is the fitted result

Table 2 Fitted parameters of curves of the resistivities, ρ_1, ρ_2, and ρ_3, versus test temperature, T, for single crystalline perovskite manganites $La_{1-x}Sr_xMnO_3$ ($x=0.2$, 0.3), where $\rho_1 = (a_{11} + a_{12}T)^3$, $\rho_2 = a_2 \exp\left(-\frac{E_2}{k_B T}\right)$,$\rho_3 = a_3 \exp\left(\frac{E_3}{k_B T}\right)$

x	a_{11} $[\Omega\ \mathrm{cm})^{1/3}]$	a_{12} $[(\Omega\ \mathrm{cm\ K^{-1}})^{1/3}]$	a_2 (Ω cm)	E_2 (eV)	T_C (K)	a_3 (Ω cm)	E_3 (eV)
0.2	0.051	3.2×10^{-4}	1.6×10^{11}	0.76	309	9.5×10^{-3}	0.0358
0.3	0.030	3.1×10^{-4}	5.0×10^{10}	0.92	369	8.3×10^{-3}	0.0001

$$\rho = \frac{(\rho_1 + \rho_2)\rho_3}{\rho_1 + \rho_2 + \rho_3} \tag{1}$$

To fit the curves of resistivity ρ vs. test temperature T, we set

$$\begin{aligned} \rho_1 &= (a_{11} + a_{12}T)^3 \\ \rho_2 &= a_2 \exp\left(-\frac{E_2}{k_B T}\right) \end{aligned} \tag{2}$$

$$\rho_3 = \rho_0 + a_3 T \tag{3}$$

where k_B is the Boltzmann constant.

Using Eqs. (1) − (3), we fitted the observed curves of ρ vs. T for the Fe, Co, and Ni metals [14] and the $Ni_{1-x}Cu_x$ ($x=0.0961$, 0.1954) alloys [15]. The fitting parameters are tabulated in Table 1, and the fitted curves are shown in Fig. 2. The fitted curves closely matched the experimental results (points).

As an example, the fitting method of the curve of ρ vs. T for Ni may be found in following:

Firstly, a linear fitting for the curve of observed resistivity ρ versus temperature T for Ni at the high temperature region was performed, as shown in Fig. 3, from which we obtained simply the parameters in Eq. (3), $\rho_0 = 15.1$ μΩ cm, and $a_3 = 0.023$ μΩ cm K^{-1}, as shown in Table 1.

Secondly, a linear fitting for the curve of observed $\rho^{1/3}$ versus temperature T for Ni at the low temperature region was performed, as shown in Fig. 4, from which we may estimate the parameters a_{11} and a_{12} in Eq. (2), $a_{11}^1 = 0.94\ (\mu\Omega\ \mathrm{cm})^{1/3}$ and $a_{12}^1 = 0.032\ \left(\mu\Omega\ \mathrm{cm\ K^{-1}}\right)^{1/3}$.

Thirdly, by adjusting the parameter values, we calculate the ρ values at different temperature using Eqs. (1) − (3) and the Origin software, to fit the curve of observed ρ versus T, again and again. Finally, we obtained the parameters a_{11}, a_{12}, a_2, and E_2, as shown in Table 1.

3 Fitting Temperature Dependences for the Resistivity of the $La_{1-x}Sr_xMnO_3$ ($x=0.2$, 0.3) Magnetic Perovskite Manganites

According to the IEO model [5–8, 12], in the $La_{1-x}Sr_xMnO_3$ ($x=0.2$, 0.3) perovskite manganites, the IEs originate from the O 2p electrons. The two electrons with opposite spin directions at the outer orbit of an O^{2-} anion may transit along the Mn–O chain and La(Sr)-O chain, respectively, forming IEs. The transition of IEs may also be described using the equivalent device shown in Fig. 1 [12]. The transition of IEs along the Mn–O chain is spin-dependent below the T_C, where resistivities ρ_1 and ρ_2 have similar characteristics to

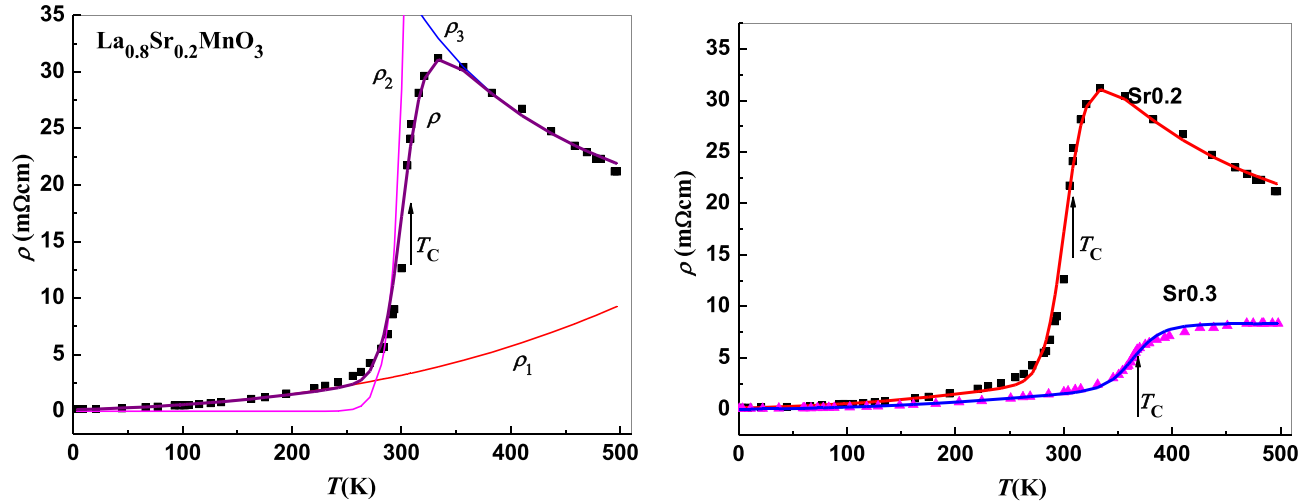

Fig. 5 Temperature dependence of resistivity ρ of single crystalline perovskite manganites $La_{1-x}Sr_xMnO_3$ ($x=0.2$, 0.3), where the curves represent the fitted results in this work, the points represent the observed results [16]

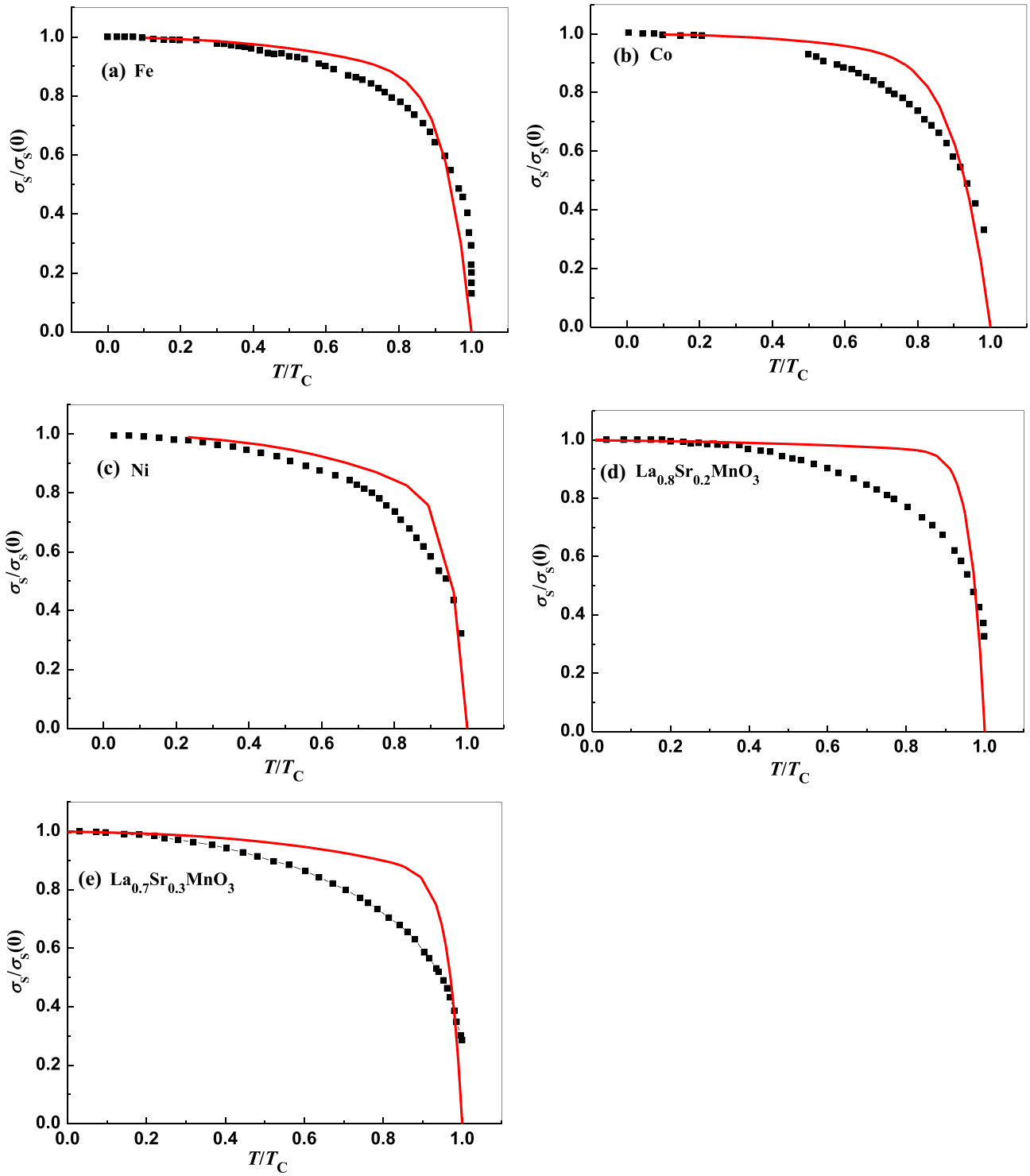

Fig. 6 Normalization magnetization $\sigma_S/\sigma_S(0)$ as function of normalization test temperature T/T_C. The curves are fitted results, $1-\rho_{12}/\rho_{12}(T_C)$, where $\rho_{12}=\rho_1+\rho_2$, the values of ρ_1 and ρ_2 originate from Figs. 2 and 5. The data points are observed results of Fe, Co, and Ni metals [14] and $La_{1-x}Sr_xMnO_3$ ($x=0.2, 0.3$) [16]

the IEs in the magnetic metals, which can be fitted using Eq. (2). The transition of IEs along the La(Sr)-O chain is spin-independent, both below and above the T_C, and may be fitted using the following equation:

$$\rho_3 = a_3 \exp\left(\frac{E_3}{k_B T}\right) \tag{4}$$

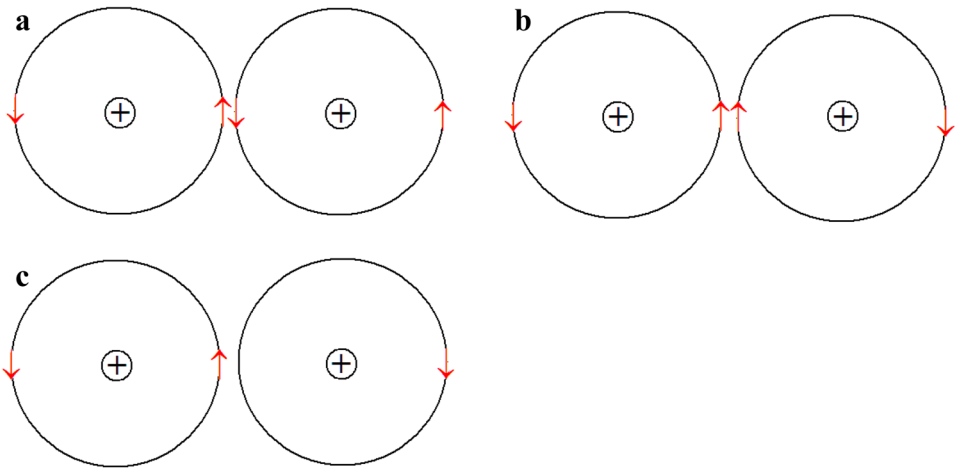

Fig. 7 Illustrations of **a** a WEP and **b, c** itinerant electrons in the outer orbits of adjacent ions [5, 6, 10]

Using Eqs. (1), (2), (4), we fitted the observed curves of ρ vs. T for $La_{1-x}Sr_xMnO_3$ ($x=0.2, 0.3$) perovskite manganites [16]. The fitting parameters are listed in Table 2, and the fitted curves are shown in Fig. 5. The fitted curves closely matched the experimental results.

As an example, the fitting method of the curve ρ vs. T for $La_{0.8}Sr_{0.2}MnO_3$ may be found in following.

For $La_{0.8}Sr_{0.2}MnO_3$, the approximate values of a_3 and E_3 in Eq. (4) may be estimated. From Eq. (4), we have

$$\ln\rho_3 = \ln a_3 + \frac{E_3}{k_B}\frac{1}{T} \tag{5}$$

Then, a linear fitting for the curve of observed $\ln\rho$ versus temperature $1/T$ for $La_{0.8}Sr_{0.2}MnO_3$ at the high temperature region was performed, and then, the approximate values of a_3 and E_3 may be calculated using the values of $\ln a_3$ and E_3/k_B. The estimation method of the parameters a_{11} and a_{12} of $La_{0.8}Sr_{0.2}MnO_3$ is similar to that of Ni. Finally, by adjusting the parameter values, we calculate the ρ values at different temperature using Eqs. (1), (2), (4) and Origin software, to fit the curve of observed ρ versus T, again and again. Therefore, we obtained the parameters a_{11}, a_{12}, a_2, E_2, a_3, and E_3, as shown in Table 2.

The fitted results in Figs. 2 and 5 indicate that the assumption for the itinerant electrons having similar properties in both magnetic metals and oxides is reasonable.

4 Fitting Temperature Dependences of the Magnetization for the Fe, Co, and Ni Magnetic Metals and the $La_{1-x}Sr_xMnO_3$ ($x=0.2, 0.3$) Magnetic Perovskite Manganites

According to the WEP model [5, 6, 10], at the ground state, two valence electrons with opposite spin directions at the outer shell in an ion (or in an ionic core in a metal) move at a constant spin direction. When two approaching electrons with the same spin direction belong to two adjacent ions, they can exchange each other, to form itinerant electrons. When two approaching electrons with opposite spin directions belong to two adjacent ions, they cannot exchange each other; as a result, a WEP is formed with a specific probability and lifetime. The energy of WEPs is the origin of the magnetic ordering energy. With T increments, the spin direction of the itinerant electrons deviates from the ground state direction, increasing the resistivity ($\rho_1+\rho_2$) of the materials; the spin directions of the electrons in a WEP deviate from the ground state direction, resulting in a decrease in the magnetic ordering energy; meanwhile, the specific saturation magnetization (σ_S) decreases.

Therefore, the dependence of σ_S on T can be discussed using the parameters obtained in the above process of fitting the curves of ρ_1 and ρ_2 vs. T. For the magnetic Fe metal, the observed normalization dependence of $\sigma_S/\sigma_S(0)$ on T/T_C is shown by the points [14] in Fig. 6a, where $\sigma_S(0)$ is the maximum specific saturation magnetization at a low temperature and T_C is the Curie temperature. Applying the fitted data of ρ_1 and ρ_2 in Fig. 2a, we set $\rho_{12}=\rho_1+\rho_2$, calculated the normalization $\rho_{12}/\rho_{12}(T_C)$ and found that the curve of $1-\rho_{12}/\rho_{12}(T_C)$ of Fe metal vs. T/T_C was close to that of $\sigma_S/\sigma_S(0)$ vs. T/T_C, as shown in Fig. 6a. This can easily be described as follows: At a low temperature, the materials have the maximum σ_S and the minimum ρ_{12}; as T increases, ρ_{12} increases slowly, and σ_S decreases slowly. Near the T_C, ρ_{12} increases rapidly and σ_S decreases rapidly. Using the same method, we obtained similar fitted results for the observed magnetizations of Co and Ni magnetic metals [14], as well as the $La_{1-x}Sr_xMnO_3$($x=0.2, 0.3$) magnetic perovskite manganites [16], as shown in Fig. 6b – e. This suggests that the spin directions deviating from the ground state are the elementary factor that affected both curves $\sigma_S - T$ and $\rho_{12} - T$, while this, in turn, indicated that the assumption regarding the magnetic ordering energy of both magnetic metals and oxides originating from the WEP energy are reasonable.

The deviation of the two curves near the T_C in Fig. 6a – e indicates that other factors affected the magnetization exist in addition to the spin directions of IEs; these require additional study in the future.

5 Conclusion

In order to understand the physical mechanism related to valence electron structure of magnetic and electrical transport of the magnetic materials, based on a set of new itinerant electron models of magnetic materials, we fitted the temperature dependences of resistivity for Fe, Co, and Ni magnetic metals, $Ni_{1-x}Cu_x$ alloys, and $La_{1-x}Sr_xMnO_3$(x=0.2, 0.3) perovskite manganites, using an equivalent device with two current-carrier channels. In the IE channel, the resistivity was fitted by $\rho_{12}=\rho_1+\rho_2$, where ρ_1 represented the resistivity originating from the transition of IEs between adjacent ions scattered by the crystal lattice; ρ_2 was the resistivity originating from the IEs, whose spin direction deviated rapidly from the ground state direction when the T was close to the T_C. Accordingly, we found that the curve of normalization $1-\rho_{12}/\rho_{12}(T_C)$ vs. T/T_C was close to the curve of normalization magnetization $\sigma_S/\sigma_S(0)$ vs. T/T_C; this was because the valence electron structure had the greatest effect on both the magnetic and electrical transport properties. At the ground state, the valence electrons at the outer shell of an ion (or the ionic core in the metals) moved in constant spin directions. When two approaching electrons with the same spin direction belong to two adjacent ions, they can exchange each other to form itinerant electrons. When two approaching electrons with the opposite spin directions belong to two adjacent ions, they cannot exchange each other; as a result, a WEP is formed with a specific probability and lifetime. The energy of WEPs is the origin of the magnetic ordering energy. As the temperature increases, the spin direction of the itinerant electrons deviates from the ground state direction; this increases the resistivity of the materials. The spin directions of the electrons in a WEP deviate from the ground state direction, resulting in a decrease in the magnetic ordering energy and, meanwhile, a decrease in the magnetization.

Appendix 1. O 2*p* itinerant electron model for magnetic oxides (IEO model)

IEO model includes the following features [5, 6]:

(i) In an oxide, O^{2-} ($2s^22p^6$) and O^{1-} ($2s^22p^5$) anions simultaneously coexist on the basis of experimental results for valence electron state. The outer orbit of an O^{1-} anion has an O 2*p* hole. In a given sublattice, an O 2*p* electron with a constant spin direction can hop from an O^{2-} anion to the O 2*p* hole of an adjacent O^{1-} anion with a metal cation acting as an intermediary.

(ii) Since an itinerant electron has a constant spin direction in a given sublattice, the two O 2*p* electrons in the outer orbit of an O^{2-} anion, which have opposite spin directions, become itinerant electrons in two different sublattices. That is, in a magnetic oxide below Curie temperature, the itinerant electrons must have opposite spin directions in two sublattices, such as (A) or [B] sites of spinel ferrites.

(iii) Subjected to the constraints of Hund's rule and that an itinerant electron has a constant spin direction in a given sublattice, the magnetic moments of the cations with 3*d* electron numbers $n_d \leq 4$ (such as Mn^{3+} or divalent/trivalent Ti or Cr cations) are antiparallel to those of the cations with $n_d \geq 5$ (such as Mn^{2+} or divalent/trivalent Fe, Co, or Ni cations), regardless of whether they are located at the (A) or [B] sublattice.

Appendix 2. Itinerant electron model for magnetic metals (IEM model)

IEM model includes the following features [5, 6]:

(i) Based on gamma radiation diffraction and other observations, in the process of forming a metal solid with a single-crystal or polycrystalline state from free atoms, most of the 4*s* electrons in 3*d* transition metals (except for Cu and Zn with a full 3*d* subshell) enter the 3*d* orbits to decrease the Pauli repulsive energy between atoms, while the remaining 4*s* electrons form free electrons.

(ii) A certain probability exists that the outer orbital 3*d* electrons transit between the outer orbits of adjacent ionic cores, forming itinerant electrons. The other 3*d* electrons are local electrons.

(iii) The resistivity of a metal decreases as the concentration of free electrons increases. The movements of free electrons are subjected by the weak crystal lattice potential field but not by the electron orbits, whose spins have no contribution to the material magnetic moment. The transition of the itinerant electrons is a spin-independent transition above the Curie temperature, but it is a spin-dependent transition below the Curie temperature, and the transition probability decreases with increasing test temperature and rapidly decreases near the Curie temperature.

Appendix 3. Weiss electron-pair (WEP) model for origin of magnetic ordering energy

WEP model includes the following features [5, 6]:

(i) Supposing that a moving electron in an outer orbit of an ion has a constant spin direction, the electrons in the outer orbits of the adjacent ions, including the adjacent cations and anions in a compound and the ions (atoms that have lost free electrons) in a metal, may have three states, as shown in Fig. 7 a, b, and c.

(ii) If the electrons have the state illustrated in Fig. 7a, there are two electrons with opposite spin directions in the outer orbit of each ion. The two electrons located between adjacent ions cannot be exchanged because they have opposite spin directions. The magnetic ordering energy is thus given by the difference between the static magnetic attractive energy and the Pauli repulsive energy of the two electrons. This type of electron pair, which has a particular lifetime and probability of appearing, is called a WEP.

(iii) When the two electrons between adjacent ions have the state shown in Fig. 7b, both the static magnetic and Pauli repulsive energies exist between the two neighboring electrons, and they can be easily exchanged since they both have the same spin direction. When the electrons have the state depicted in Fig. 7c, the middle electron can easily transit to the outer orbit of the right ion. Thus, both the electron exchange in Fig. 7b and electron transit in Fig. 7c may be considered to be simply the transitions of itinerant electrons, wherein the spin directions of the itinerant electrons cannot change.

Acknowledgements The authors would like to thank Enago (www.enago.cn) for the English language review.

Funding This work was supported by the National Natural Science Foundation of China (Grant No. NSF-11174069) and the Doctor Foundation of Hebei Normal University (L2022B10).

Declarations

Conflict of Interest The authors declare no competing interests.

References

1. Dai, D.S., Qian, K.M.: Ferromagnetism (in Chinese). Science Press, Beijing (1987)
2. Coey, J.M.D.: Magnetism and magnetic materials. Cambridge University Press, Cambridge (2010)
3. Chikazumi, S.: Physics of Ferromagnetism (2e). Oxford University Press, London (1997)
4. Stöhr, J., Siegmann, H.C.: Magnetism: From Fundamentals to Nanoscale Dynamics. Springer, Berlin Heidelberg, New York (2006)
5. Tang, G.D.: New Itinerant Electron Models of Magnetic Materials. Science Press, Beijing, and Springer Nature, Singapore (2021)
6. Tang, G.D., Li, Z.Z., Ma, L., Qi, W.H., Wu, L.Q., Ge, X.S., Wu, G.H., Hu, F.X.: Phys. Rep. **758**, 1–56 (2018)
7. Xu, J., Ma, L., Li, Z.Z., Lang, L.L., Qi, W.H., Tang, G.D., Wu, L,Q., Xue, L.C., Wu, G.H.: Physica. Status. Solidi. B. **252**, 2820 (2015)
8. Wu, L.Q., Qi, W.H., Ge, X.S., Ji, D.H., Li, Z.Z., Tang, G.D., Zhong, W.: Europhys. Lett. **120**, 27001 (2017)
9. Qi, W.H., Ma, L., Li, Z.Z., Tang, G.D., Wu, G.H.: Acta Phys. Sin. **66**, 027101 (2017)
10. Qi, W.H., Li, Z.Z., Ma, L., Tang, G.D., Wu, G.H., Hu, F.X.: Acta. Phys. Sin. **66**, 067501 (2017)
11. Qi, W.H., Li, Z.Z., Ma, L., Tang, G.D., Wu, G.: H. AIP Adv. **8**, 065105 (2018)
12. Qian, J.J., Qi, W.H., Li, Z.Z., Ma, L., Tang, G.D., Du, Y.N., Chen, M.Y., Wu, G.H., Hu, F.X.: RSC Adv. **8**, 4417–4425 (2018)
13. Li, Z.Z., Qi, W.H., Ma, L., Tang, G.D., Wu, G.H., Hu, F.X.: J. Magn. Magn. Mater. **482**, 173–177 (2019)
14. Wijn, H.P.J.: Magnetic properties of Metals, Subvolume a. Springer-Verlag Berlin Heidelberg, Berlin, p120 (1986)
15. Fang, J.X., and Lu, D.: Solid state physics (in chinese). Shanghai Scientific and Technical Publishers, pp. 310–315 (1981)
16. Urushibara, A., Moritomo, Y., Arima, T., Asamitsu, A., Kido, G., Tokura, Y.: Phys. Rev. B **51**, 14103 (1995)